

## Research Article

# Metabolite Profiling of the Environmental-Controlled Growth of *Marsilea crenata* Presl. and Its *In Vitro* and *In Silico* Antineuroinflammatory Properties

Burhan Ma'arif<sup>1\*</sup> Faisal Akhmal Muslikh<sup>2</sup> Dilla Amalia<sup>1</sup>Anisah Mahardiani<sup>1</sup> Luthfi Achmad Muchlasi<sup>1</sup>Pramudita Riwanti<sup>3</sup> Maximus Markus Taek<sup>4</sup> Hening Laswati<sup>5</sup> Mangestuti Agil<sup>6</sup> 

<sup>1</sup> Department of Pharmacy, Universitas Islam Negeri Maulana Malik Ibrahim, Malang, East Java, Indonesia

<sup>2</sup> Master Program of Pharmaceutical Science, Universitas Airlangga, Surabaya, East Java, Indonesia

<sup>3</sup> Department of Pharmacy, Universitas Hang Tuah, Surabaya, East Java, Indonesia

<sup>4</sup> Department of Chemistry, Universitas Katolik Widya Mandira, Kupang, East Nusa Tenggara, Indonesia

<sup>5</sup> Department of Physical Medicine and Rehabilitation, Universitas Airlangga, Surabaya, East Java, Indonesia

<sup>6</sup> Department of Pharmaceutical Science, Universitas Airlangga, Surabaya, East Java, Indonesia

\*email: [burhan.maarif@farmasi.uin-malang.ac.id](mailto:burhan.maarif@farmasi.uin-malang.ac.id)

**Keywords:**

Environmental-controlled growth  
HMC3 microglia cells  
*Marsilea crenata* Presl.  
Neuroinflammatory  
Phytoestrogens

**Abstract**

This study was aimed to evaluate the metabolite contents and antineuroinflammatory potential of *Marsilea crenata* Presl. grown under a controlled environmental condition. The antineuroinflammatory test has been carried out *in vitro* using ethanolic extract of *M. crenata* leaves on HMC3 microglia cells. An *in silico* approach was applied to predict the active compounds of the extract. The HMC3 microglia cells were induced with IFN $\gamma$  to create prolonged inflammatory conditions and then treated with 96% ethanolic extract of the *M. crenata* leaves of 62.5, 125, and 250  $\mu$ g/mL. The expression of MHC II was analyzed using the ICC method with the CLSM instrument. Metabolites of the extract were profiled using UPLC-QToF-MS/MS instrument and MassLynx 4.1 software. *In silico* evaluation was conducted with molecular docking on 3OLS protein using PyRx 0.8 software, and physicochemical properties of the compounds were analyzed using SwissADME webtool. The ethanolic extract of *M. crenata* leaves could reduce the MHC II expression in HMC3 microglia cells in all concentrations with the values 97.458, 139.574, and 82.128 AU. The result of metabolite profiling found 79 compounds in the extract. *In silico* evaluation showed that 19 compounds gave agonist interaction toward 3OLS, and three met all parameters of physicochemical analysis. The ethanolic extract of the environmental-controlled growth of *M. crenata* leaves antineuroinflammatory activity on HMC3 microglia cells. The extract was predicted to contain some phytoestrogen compounds which act as 3OLS agonists.

Received: February 8<sup>th</sup>, 2022

1<sup>st</sup> Revised: May 13<sup>th</sup>, 2022

2<sup>nd</sup> Revised: July 3<sup>rd</sup>, 2022

3<sup>rd</sup> Revised: July 27<sup>th</sup>, 2022

Accepted: July 31<sup>th</sup>, 2022

Published: August 31<sup>th</sup>, 2022



© 2022 Burhan Ma'arif, Faisal Akhmal Muslikh, Dilla Amalia, Anisah Mahardiani, Luthfi Achmad Muchlasi, Pramudita Riwanti, et al. Published by Institute for Research and Community Services Universitas Muhammadiyah Palangkaraya. This is an Open Access article under the CC-BY-SA License (<http://creativecommons.org/licenses/by-sa/4.0/>). DOI: <https://doi.org/10.33084/bjop.v5i3.3262>

## INTRODUCTION

The prevalence of postmenopausal women worldwide is gotten higher over several decades<sup>1</sup>. This increase is closely related to a direct decline in quality of life<sup>2,3</sup>. Women in the postmenopause phase will experience various disease complaints caused by estrogen deficiency conditions, one of which is a neurodegenerative disorder<sup>4</sup>.

Neuroinflammation is one of the leading causes of neurodegenerative disorders arising from estrogen deficiency<sup>5,6</sup>. Neuroinflammation occurs due to an increase in activated microglia in the M1 polarization situation so that it can increase the expression of proinflammatory signaling factors such as major histocompatibility complex II (MHC II) and other inflammatory cytokines such as interleukin-1 (IL-1), interleukin-6 (IL-6), tumor necrosis factor- $\alpha$  (TNF- $\alpha$ ), and nitric oxide (NO) in the brain<sup>7,8</sup>. Increased inflammatory cytokines will reduce synapsis and plasticity functions of neuron cells and induce cell death<sup>9</sup>.

Celecoxib, ibuprofen, minocycline, and aspirin are some medicines used to treat neuroinflammation<sup>10,11</sup>. However, those medicines appear with potential side effects in the form of gastrointestinal tract (GIT) disorders such as nausea, gastritis, abdominal pain, and digestive tract bleeding, as well as other side effects such as dizziness, hypertension, headache, and vertigo<sup>12-14</sup>. These side effects encourage the need for various studies on potential new drug sources with minimal side effects, such as phytoestrogens<sup>15-18</sup>. Phytoestrogens are a group of natural plant products with a structure and function similar to 17 $\beta$ -estradiol<sup>19-21</sup>.

*Marsilea crenata* Presl. is one of the plants used as the typical food by the local community in East Java, Indonesia<sup>22</sup>. Ethanol 96% extract of *M. crenata* leaves been tested by radioimmunoassay (RIA) and shows a high estrogen-like substance<sup>23</sup>. Other previous studies also have shown that this plant contains phytoestrogen group compounds, such as flavonoids, that can act as an anti-inflammatory and has other estrogenic activity for maintaining human body homeostasis<sup>24-28</sup>.

In this research, we cultivated *M. crenata* under external controlled factors to gain a standardized raw material of this plant. Cultivation was carried out in Kediri, East Java, Indonesia. This area is a lowland of 0-200 m above sea level (masl), with humidity of 60-90% and an average temperature of 23.8-30.7°C<sup>29</sup>. The plant was cultivated in a greenhouse under controlled nutrition, soil, irrigation, and some environmental factors, to produce better quality and quantity of the raw material of this plant<sup>30-33</sup>.

This study aimed to prove the antineuroinflammatory activity of the 96% ethanolic extract of the leaves of *M. crenata* grown under controlled environmental conditions in inhibiting HMC3 microglia cells. This inhibition was observed in the situation of M1 polarization of these cells, with a decrease of MHC II expression as an indicator. This study also aimed to predict phytoestrogen compounds that play a role in the antineuroinflammatory activity through metabolite profiling using ultra-performance liquid chromatography – quadrupole time of flight – mass spectrometry (UPLC-QToF-MS/MS) and *in silico* studies of those compounds on estrogen receptors  $\beta$  (ER $\beta$ ), which, in this case using protein 3OLS from protein data bank (PDB).

## MATERIALS AND METHODS

### Materials

#### Plant materials

The leaves of *M. crenata* were harvested from a controlled farming (greenhouse) in Kediri, East Java, Indonesia. The characteristics of the plants were two weeks old, the stem height was approximately 17 cm, the leaf width was approximately 2 cm, and the color of the leaves was dark green. The leaves were then identified at Unit Pelayanan Teknis (UPT) Materia Medika, Batu, East Java, Indonesia, with the determination key of 1a-17b-18a-1 and identification letter 074/368/102.7/2017. The specification of the cultivation area and the external factors are listed in **Table I**.

**Table I.** Specification of location and external factors in the cultivation of *M. crenata*

Parameter	Value
Region	Pagu, Kediri, East Java, Indonesia
Height	Lowland, 0-200 masl
Rainfall	130-150 mm per year, with the rainy day number average for 6-15 days
Climate	Tropical with 2 seasons
Temperature	Average maximum temperature of 30.7°C Average minimum temperature of 23.8°C Annual average temperature of 27.2°C
Humidity	60-90%
Irrigation	Ground water
Growing Media	Not submerged with water
Fertilizer	Organic fertilizer with specification: C Organic $\geq$ 15% C/N Ratio : 15-25 pH : 4-9 Water Content : 8-20%
Plantation Location	Green house

### Chemicals

Fetal bovine serum (FBS), penicillin, streptomycin, Eagle's minimum essential medium (EMEM), dimethyl sulfoxide (DMSO), tween 80, phosphate-buffered saline (PBS), paraformaldehyde (PFA), bovine serum albumin (BSA), fluorescein isothiocyanate (FITC) anti-rabbit secondary antibody were purchased from Sigma-Aldrich (St. Louis, USA). MHC II anti-rabbit secondary antibody was purchased from Abcam (Cambridge, UK). Ethanol 96%, dichloromethane, methanol, acetonitrile, and formic acid were purchased from Merck (Darmstadt, Germany).

### Hardware and software

The hardware used was an A416MA-EB422TS personal computer with Intel Celeron. The software used is the operating system Windows® 10. ChemDraw Ultra 12.0 was used in drawing 2D structures. Avogadro 1.0.1 was used in structural optimization. The docking process was done with AutoDock Vina using PyRx 0.8. Visualization of docking results was performed using Biovia Discovery Studio 2016.

### Methods

#### Extraction

About 500 g of powdered leaves of *M. crenata* were extracted with 96% ethanol using the ultrasonic method with Soltec Sonica 5300EP S3 for 3 x 10 minutes, filtered, and evaporated at 50°C using a Heidolph G3 rotary evaporator. A 25 g of the 96% ethanolic extract was obtained and subjected to further test and analysis.

#### Cell culture

HMC3 microglia cells (ATCC® CRL-3304™) were cultured using complete media in 25 cm<sup>2</sup>-sized flasks which contained 10% of FBS and a mixture of 1% of penicillin-streptomycin in a  $\pm$ 5 mL media EMEM. Cells in the flask were then incubated in a 5% CO<sub>2</sub> ThermoScientific Hera Cell 150i incubator at 37°C for a week. The cells were then placed into a 24-well microplate after the confluence was approximately 80%.

#### Measurement of MHC II expression

As much as 40 mg of the 96% ethanolic extract was suspended in the mixture of 0.5% DMSO and 0.5% Tween 80 to produce the mother liquor of 4,000  $\mu$ g/mL; it was then diluted in the concentration of 62.5; 125; 250  $\mu$ g/mL. About 40  $\mu$ L of genistein was added with the culture media reaching 0.8 mL to produce genistein with the concentration of 50  $\mu$ M, which was used as the positive control. Induction of IFN- $\gamma$  was performed after cells were cultured on a 24-well microplate and reached 80% confluence. After induction of 10 ng IFN- $\gamma$  for 24 hours, the cells were rinsed with PBS and then treated with 50  $\mu$ M genistein for 48 hours. The cells were then fixated with 4% PFA, Triton X-100, and blocking buffer, and also primary and secondary antibodies were added. They were, afterward, rinsed using PBS and visualized MHC II with CLSM (Olympus Fluoview Ver. 4.2a.) 488 nm<sup>34</sup>.

### Metabolite profiling

The process of metabolite profiling was conducted at Pusat Laboratorium Forensik Badan Reserse Kriminal Kepolisian Negara Republik Indonesia (Puslabfor Bareskrim Polri) by using UPLC-QToF-MS/MS instrument. 96% ethanolic extract was prepared using dichloromethane and methanol solvents through the solid phase extraction (SPE) method. After that, 5  $\mu$ L was equally injected into ACQUITY UPLC® H-Class System (Waters, USA) with the detector of MS Xevo G2-S QToF (Waters, USA). Samples were separated in the column of ACQUITY BEH C18 (1.7  $\mu$ m  $\times$  2.1 mm  $\times$  50 mm) with acetonitrile of + 0.05% of formic acid and water + 0.05% of formic acid as the mobile phase, with the flow rate of 0.2 mL/minute. The analysis result of UPLC-QToF-MS/MS was processed using MassLynx 4.1 software to get chromatogram data and m/z spectrum from each detected peak. The detected compounds were then confirmed using the online database of ChemSpider (<http://www.chemspider.com>), PubChem (<https://pubchem.ncbi.nlm.nih.gov>), and MassBank (<https://massbank.eu/MassBank>).

### In silico study

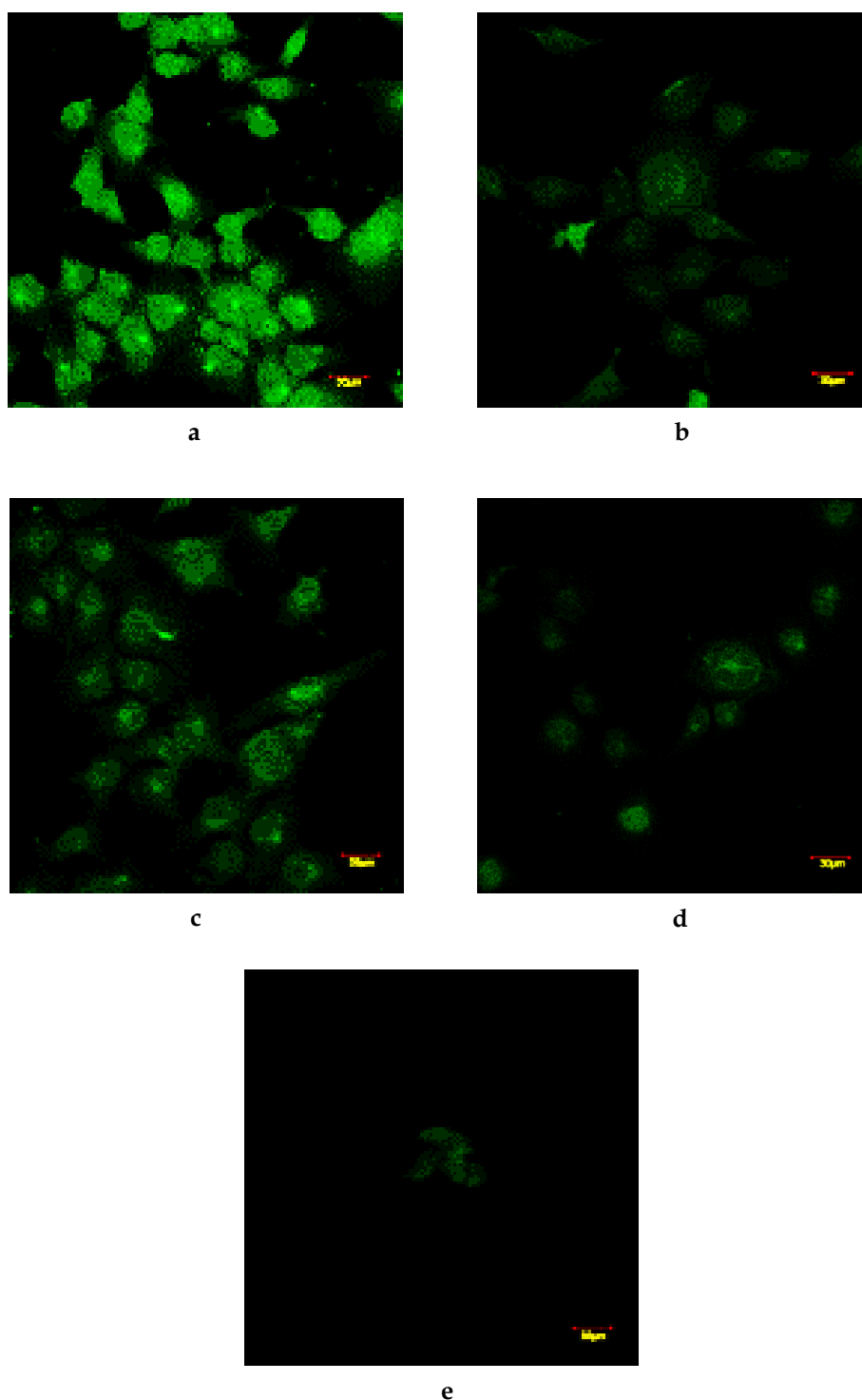
X-ray protein from ER $\beta$  was attained from the protein data bank (<http://www.rcsb.org>) with the PDB ID 3OLS. The antineuroinflammatory impact to be evaluated in this study is the antineuroinflammatory effect that emerges from phytoestrogens in plants, replacing the role of estrogen in the ER-dependent pathway and not through other mechanisms. ER $\beta$  also has a higher amount than other receptors, is more sensitive to estrogen binding, and plays the most role in regulating nerve cell homeostasis<sup>35,36</sup>.

The initial preparation was performed to separate native ligand (17 $\beta$ -estradiol) from 3OLS protein using Biovia Discovery Studio Visualizer 2016 and saved in Sybyl mol2 format. Metabolite profiling compounds drawn 2D using ChemDraw Ultra 12.0 and saved in mol format. Internal validation was performed by adding 3OLS and 17-estradiol ligands and then docking them with PyRx 0.8 software. Native ligand and the result compounds of metabolite profiling were then optimized with Avogadro 1.0.1 using the MMFF94 method. Then, molecular docking was conducted using PyRx 0.8 with the AutoDock Vina method to simulate the docking process. All compound files were imported into the PyRx 0.8 software and converted to pdbqt format automatically. The determination of the grid box includes setting location according with grid center  $x = 11.1148$ ,  $y = -35.813$ , and  $z = 12.1403$  with dimension of  $25 \times 25 \times 25$  Å. Setting the exhaustiveness to number 8 and the work grid through Autogrid to 17-estradiol ligand completed the operation, yielding a binding affinity value and a molecular docking compound in the form of pdbqt. The result of complex visualization between receptor and ligand was observed using Biovia Discovery Studio Visualizer 2016 to see the interaction that occurred. To see the compound's potential as oral medicine, then the compounds which had the agonist interaction were processed with physicochemical analysis using the SwissADME web tool to find out the penetration capability.

## RESULTS AND DISCUSSION

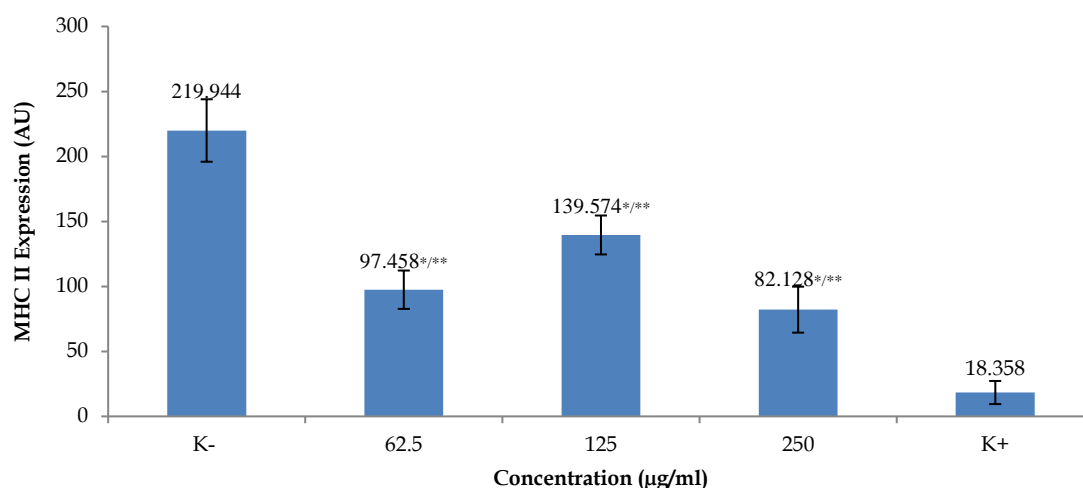
### Measurement of MHC II expression

**Figure 1** was the visualization result using the CLSM instrument, which displayed MHC II fluorescence intensity in the figure. IFN $\gamma$  induction for 24 hours can activate nuclear factor kappa B (NF- $\kappa$ B) through toll-like receptor 4 (TLR4), which can affect cell protein synthesis, so that it can activate the microglia in M1 polarization and change its morphology into amoeboid, which cause the appearance of the inflammatory mediator, one of them is MHC II<sup>16,17,37,38</sup>. IFN $\gamma$  plays the role of activating the microglia and can increase MHC II molecule expression as the transcription activator. MHC II plays a role in producing the exogen antigen, activating the T helper cell through the receptor, and secreting several cytokines to manage the immune response<sup>39,40</sup>. The strongest intensity was seen on the negative control, and the weakest intensity was seen on the positive control. In the negative control, treatment was not given, so it caused the HMC3 microglia cells to stay active on M1 polarization and produced high MHC II fluorescence intensity. All treatment groups showed lower MHC II fluorescence intensity compared to the negative control.



**Figure 1.** MHC II fluorescence intensity on HMC3 microglia cells (a) negative control; (b) 62.5 µg/mL; (c) 125 µg/mL; (d) 250 µg/mL; and (e) genistein.

Furthermore, **Figure 2** shows MHC II expressions comparison in the concentration of 62.5; 125; 250 µg/mL with negative control and positive control. In all concentrations, MHC II expression was lower compared to the negative control. The result of ANOVA test showed significant difference in MHC II expression reduction among all concentrations on negative control ( $p=0.000$ ;  $p=0.000$ ; and  $p=0.000$ ) and on positive control ( $p=0.000$ ;  $p=0.000$ ; and  $p=0.000$ ).



**Figure 2.** Expression of MHC II in 96% ethanol extract of *M. crenata* leaves. The \* sign indicates a significant difference from the negative control (K-), while the \*\* sign indicates a significant difference from the positive control (K+).

In **Figure 2**, concentration increase was not accompanied by MHC II expression decrease. This probably happened because of the Non-Monotonic Dose Response (NMDR) phenomenon in HMC3 microglia cells, which was indicated by various slope values in the given concentration ranges<sup>41</sup>. NMDR often occurred in research by using hormone treatment or sample used as the hormone substitute, in this case, was phytoestrogen compound in 96% ethanol extract of the environmental controlled growth *M. crenata* leaves.

The affinity level difference between the hormone or sample that substituted the hormone and the receptor could cause difficulty in predicting the response following the increased concentration. Another factor causing NMDR was receptor downregulation and receptor desensitization; this may happen because the increasing concentration on the sample could cause the compound to bond with other receptors except for ER or make ER insensitive in bonding with the compound. However, the moment the concentration was continuously increased, it could increase the number of ER degraded and unequal to the produced ER, which caused the cell to produce ER massively and could increase the bond of the compound with ER and the activity response<sup>41,42</sup>.

A 62.5 µg/mL concentration was the optimum concentration for reducing MHC II fluorescence intensity. This was because the concentration treatment showed a significant difference from the negative control and a big fluorescence intensity difference between the negative control value and the MHC II expression value of 97.458 Arbitrary Unit (AU). Concentrations 62.5 and 250 µg/mL were the concentrations that also could reduce MHC II expression well but did not differ from each other significantly in statistics, so 62.5 µg/mL was chosen as the most optimum concentration because the small concentration could produce a similar effect with the concentration of 250 µg/mL. The result showed that giving 96% ethanol extract to the controlled environmental growth of *M. crenata* leaves treatment reduced the number of MHC II, which was observed from the expression reduction.

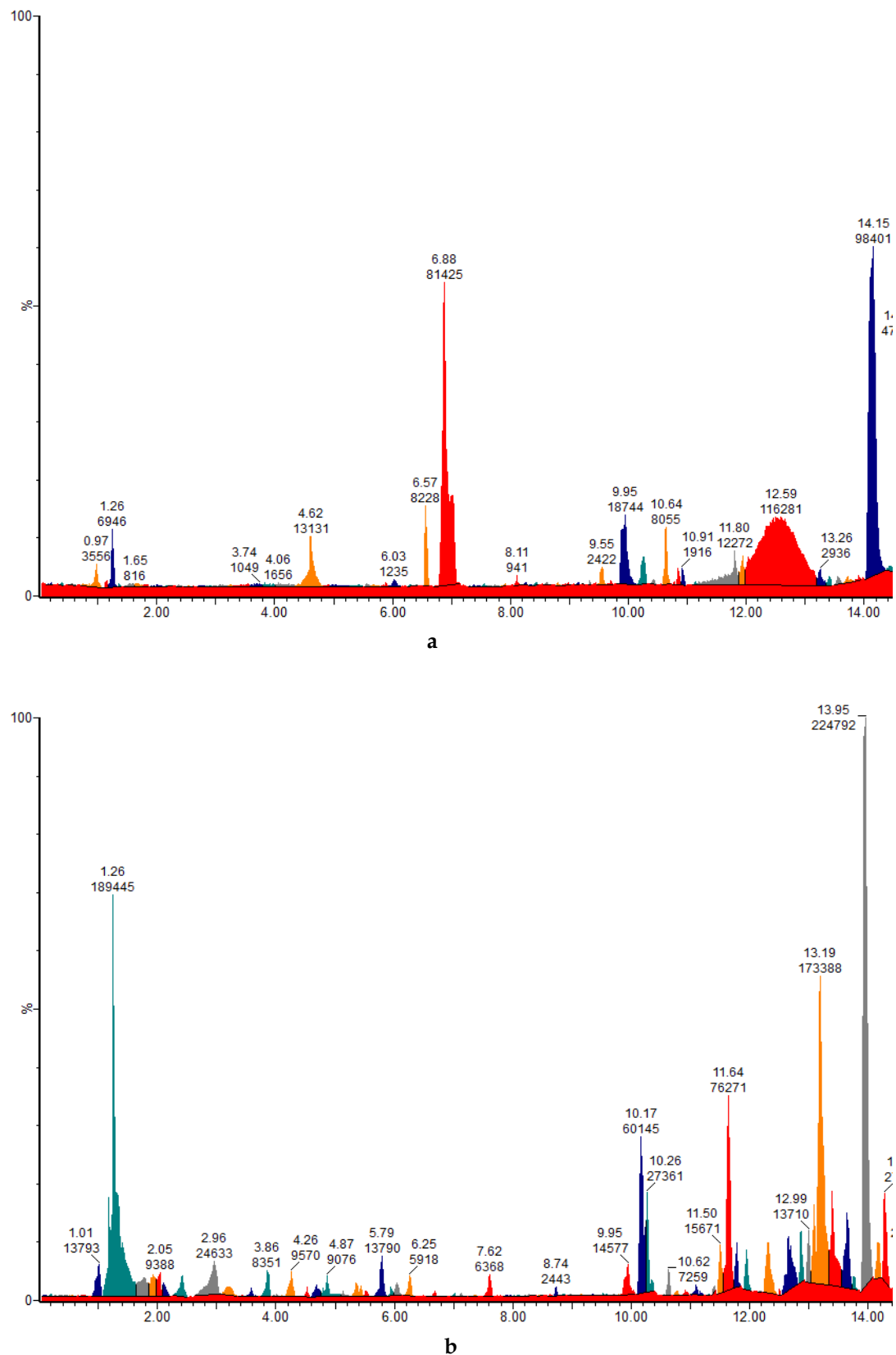
This *in vitro* activity test was carried out to know the activity potential of a plant that was given to a cell<sup>43</sup>. The result of the *in vitro* test showed that the 96% ethanol extract of *M. crenata* leaves had antineuroinflammatory activity, which was indicated by a significant MHC II expression decrease. Then, to predict the compound contained in 96% ethanol extract of *M. crenata* leaves, metabolite profiling was conducted<sup>44</sup>, and to predict the compound which had antineuroinflammatory activity, *in silico* analysis was carried out<sup>45</sup>.

#### Metabolite profiling

The metabolite profiling result of 96% ethanol extract of the controlled environmental growth of *M. crenata* leaves by using UPLC-QToF-MS/MS instrument on dichloromethane and methanol solvents in the form of total ion chromatogram (TIC)

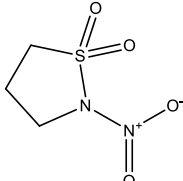
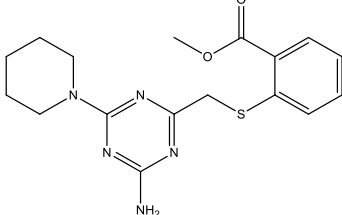
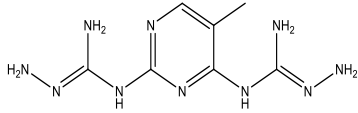
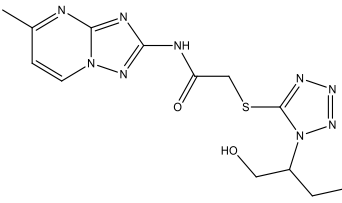
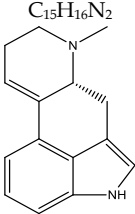
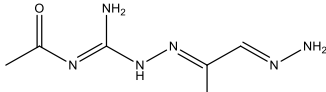
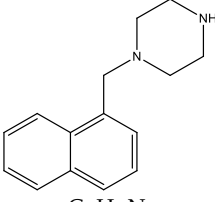
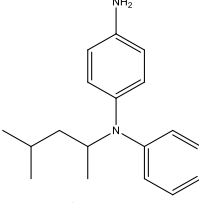



can be seen in **Figure 3**. In contrast, the value of retention time (RT), % area, m/z, molecule formula, and the compound's name can be overviewed in **Tables II** and **III**.

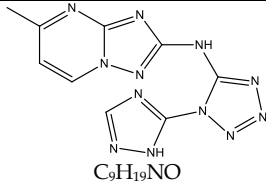
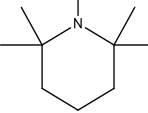
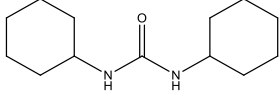
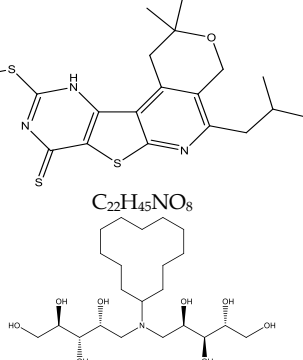


**Figure 3.** TIC of 96% ethanol extract of *M. crenata* leaves in solvent (a) dichloromethane and (b) methanol.

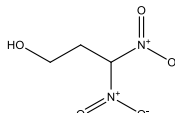
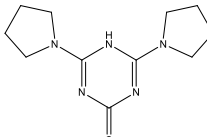
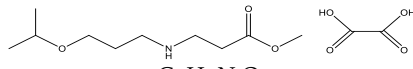
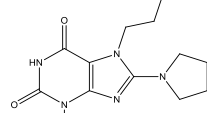
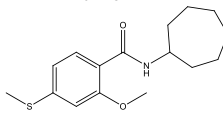
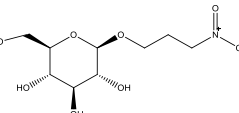
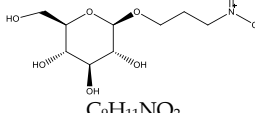
**Table II.** Prediction of compounds in 96% ethanol extract of *M. crenata* leaves in dichloromethane solvent

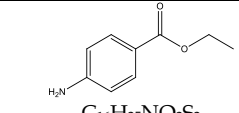
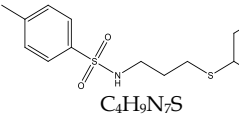
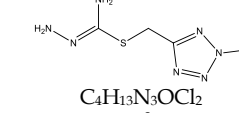
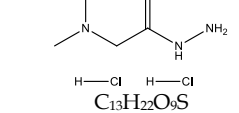
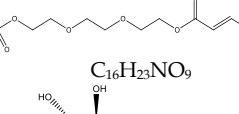
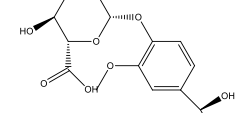
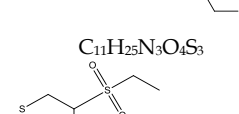
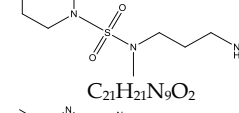
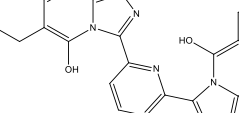
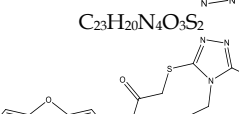
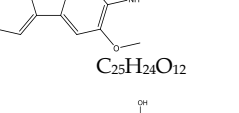
No.	RT (min)	% Area	m/z	Molecular Formula and Structure	Compound Name
1	0.971	0.8040	166.0053	$C_3H_6N_2O_4S$ 	2-Nitro-1,2-thiazolidine 1,1-dioxide
2	1.255	1.5705	359.1417	$C_{17}H_{21}N_5O_2S$ / 	Methyl 2-([4-amino-6-(1-piperidinyl)-1,3,5-triazin-2-yl]methyl)sulfanyl)benzoate
3	4.058	0.3745	238.1403	$C_7H_{14}N_{10}$ 	N'',N''''-(5-Methyl-2,4-pyrimidinediyl)dicarbonohydrazonic diamide
4	5.554	0.0696	363.1224	$C_{13}H_{17}N_9O_2S$ 	2-([1-(1-Hydroxy-2-butanyl)-1H-tetrazol-5-yl]sulfanyl)-N-(5-methyl[1,2,4]triazolo[1,5-a]pyrimidin-2-yl)acetamide
5	6.028	0.3691	224.1309	$C_{15}H_{16}N_2$ 	6-Methyl-9,10-didehydroergoline
6	6.407	0.0311	184.1070	$C_6H_{12}N_6O$ 	N-(E)-Amino[2-(1-hydrazono-2-propanylidene)hydrazino]methylene)acetamide
7	6.882	20.2706	226.1475	$C_{15}H_{18}N_2$ 	1-(1-Naphthylmethyl) piperazine
8	8.115	0.2128	268.1938	$C_{18}H_{24}N_2$ 	N-(4-Methyl-2-pentanyl)-N-phenyl-1,4-benzenediamine
9	9.548	0.5447	284.0996	$C_9H_8N_{12}$ 	5-Methyl-N-[1-(1H-1,2,4-triazol-5-yl)-1H-tetrazol-5-yl][1,2,4]triazolo[1,5-a]pyrimidin-2-amine

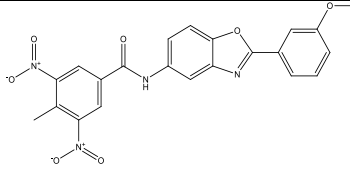
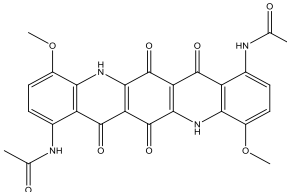
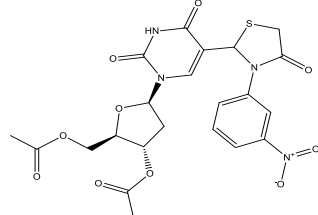
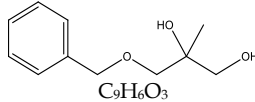
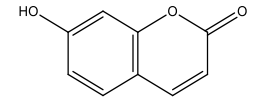
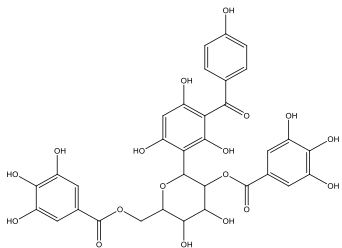
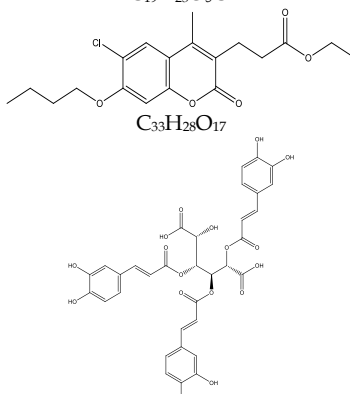
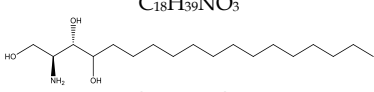
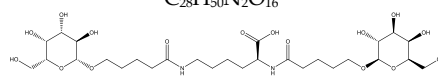


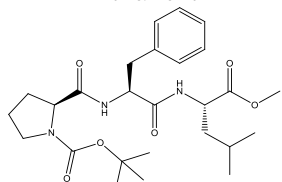

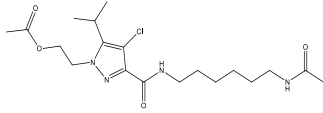
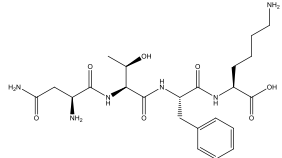
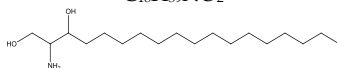
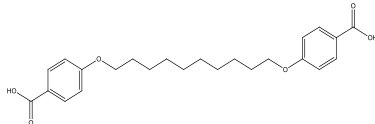
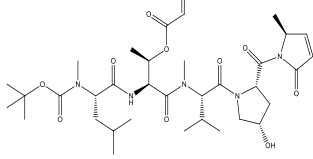
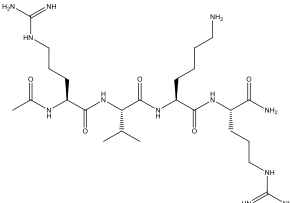
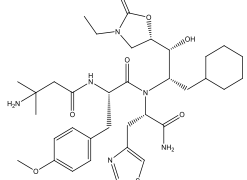
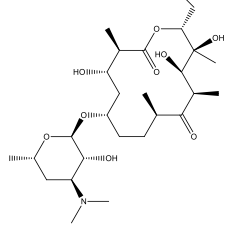

10	10.243	1.2945	157.1468	 $C_9H_{19}NO$	2,2,6,6-Tetramethyl-4-piperidinol
11	10.422	0.1290	224.1886	 $C_{13}H_{24}N_2O$	1,3-Dicyclohexylurea
12	13.256	0.6638	405.1003	 $C_{19}H_{23}N_3OS_3$	5-Isobutyl-2,2-dimethyl-10-(methylsulfanyl)-1,4-dihydro-2H-pyrano[4'',3'':4',5']pyrido[3',2':4,5]thieno[3,2-d]pyrimidine-8(11H)-thione
13	13.551	0.2674	451.3150	 $C_{22}H_{45}NO_8$	(2R,3S,4R,2'R,3'S,4'R)-5,5'-(Cyclododecylimino)di(1,2,3,4-pentanetetrol)

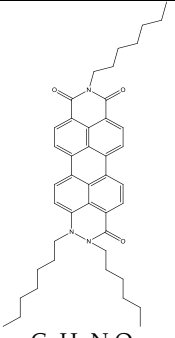
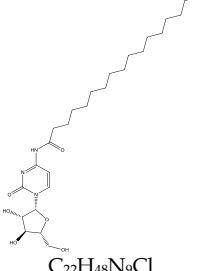
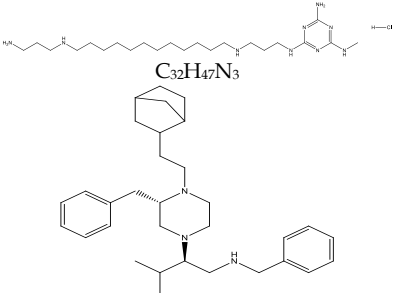
**Table III.** Prediction of compounds in 96% ethanol extract of *M. crenata* leaves in methanol solvent

No.	RT (min)	%Area	m/z	Molecular Formula and Structure	Compound Name
1	1.013	1.1178	150.0282	 $C_3H_6N_2O_5$	3,3-Dinitro-1-propanol
2	1.255	15.3535	235.1431	 $C_{11}H_{17}N_5O$	4,6-Di(1-pyrrolidinyl)-1,3,5-triazin-2(5H)-one
3	1.930	0.8740	293.1473	 $C_{12}H_{23}NO_7$	Methyl N-(3-isopropoxypropyl)- $\beta$ -alaninate ethanedioate (1:1)
4	2.046	0.7608	293.1491	 $C_{13}H_{19}N_5O_3$	7-(2-Methoxyethyl)-3-methyl-8-(1-pyrrolidinyl)-3,7-dihydro-1H-purine-2,6-dione
5	2.109	0.3141	293.1454	 $C_{16}H_{23}NO_2S$	N-Cycloheptyl-2-methoxy-(methylsulfanyl)benzamide
6	2.425	0.7979	267.0956	 $C_9H_{17}NO_8$	Miserotoxin
7	2.962	1.9964	165.0790	 $C_9H_{11}NO_2$	Benzocaine

8	3.183	0.4959	327.1324		N-[3-(Cyclohexylsulfanyl) propyl]-4-methylbenzene sulfonamide
9	3.858	0.6768	187.0639		(2-Methyl-2H-tetrazol-5-yl)methyl carbamo hydrazonothioate
10	4.016	0.0231	189.0435		Girard Reagent D dihydrochloride
11	4.258	0.7756	354.0980		2,2-Dioxido-3,6,9-trioxa-2λ6-thiaundecan-11-yl ethyl (2E)-2-butenedioate
12	4.532	0.1558	373.1070		(-)-Metanephrine glucuronide
13	4.870	0.7356	359.1002		3-(Ethylsulfonyl)-N-methyl-N-[3-(methylamino)propyl]-4-thiomorpholinesulfonamide
14	5.133	0.0955	431.1820		3,3'-(2,6-Pyridinediyl)bis(6-ethyl-7-methyl[1,2,4]triazolo [4,3-a]pyrimidin-5-ol)
15	5.354	0.4942	464.0975		2-[[4-Ethyl-5-(2-thienyl)-4H-1,2,4-triazol-3-yl]sulfonyl]-N-(2-methoxydibenzo[b,d]furan-3-yl)acetamide
16	5.533	0.1073	516.1268		1,3-Bis{[(2E)-3-(3,4-dihydroxy phenyl)-2-propenoyl]oxy}-4,5-dihydroxycyclohexane carboxylic acid
17	5.786	1.1176	498.1174		(1S,4S)-1,4-Dihydronaphthalene-1,4-diylbis(methylene) bis(4-methylbenzenesulfonate)
18	5.944	0.1634	448.1023		N-[2-(3-Methoxyphenyl)-1,3-benzoxazol-5-yl]-4-methyl-3,5-dinitrobenzamide

19	6.049	0.3460	516.1278	 <chem>C<sub>26</sub>H<sub>20</sub>N<sub>4</sub>O<sub>8</sub></chem>	N,N'-(4,11-Dimethoxy-6,7,13,14-tetraoxo-5,6,7,12,13,14-hexahydroquinolino[2,3-b]acridine-1,8-diyl)diacetamide
20	6.249	0.4796	534.1054	 <chem>C<sub>22</sub>H<sub>22</sub>N<sub>4</sub>O<sub>10</sub>S</chem>	3',5'-Di-O-acetyl-2'-deoxy-5-[3-(3-nitrophenyl)-4-oxo-1,3-thiazolidin-2-yl]uridine
21	6.682	0.1119	196.1099	 <chem>C<sub>11</sub>H<sub>16</sub>O<sub>3</sub></chem>	3-(Benzyloxy)-2-methyl-1,2-propanediol
22	7.019	0.0473	162.0317	 <chem>C<sub>9</sub>H<sub>6</sub>O<sub>3</sub></chem>	Umbelliferone
23	7.124	0.0409	712.1271	 <chem>C<sub>33</sub>H<sub>28</sub>O<sub>18</sub></chem>	1,5-Anhydro-2,6-bis-O-(3,4,5-trihydroxybenzoyl)-1-[2,4,6-trihydroxy-3-(4-hydroxybenzoyl)phenyl]hexitol
24	7.345	0.0231	366.1232	 <chem>C<sub>19</sub>H<sub>23</sub>O<sub>5</sub>Cl</chem>	Ethyl 3-(7-butoxy-6-chloro-4-methyl-2-oxo-2H-chromen-3-yl)propanoate
25	7.619	0.5161	696.1328	 <chem>C<sub>33</sub>H<sub>28</sub>O<sub>17</sub></chem>	3,4,5-Tris-O-[(2E)-3-(3,4-dihydroxyphenyl)-2-propenoyl]-D-glucaric acid
26	10.264	2.2174	317.2935	 <chem>C<sub>18</sub>H<sub>39</sub>NO<sub>3</sub></chem>	(2S,3S)-2-Amino-1,3,4-octadecanetriol
27	10.622	0.5883	670.3158	 <chem>C<sub>28</sub>H<sub>50</sub>N<sub>2</sub>O<sub>16</sub></chem>	(2S)-2,6-Bis[(5-[(2R,3R,4S,5R,6R)-3,4,5-trihydroxy-6-(hydroxymethyl) tetrahydro-2H-pyran-2-yl]oxy]pentanoyl)amino]hexanoic acid

28	10.781	0.0919	489.2842	$C_{26}H_{39}N_3O_6$ 	Methyl 1-[(2-methyl-2-propyl)oxy]carbonyl]propylphenylalanyl leucinate
29	10.906	0.1012	241.2775	$C_{16}H_{35}N$ 	Cetylamine
30	11.085	0.2922	414.2036	$C_{19}H_{31}N_4O_4Cl$ 	2-[3-[(6-Acetamido)hexyl] carbamoyl]-4-chloro-5-isopropyl-1H-pyrazol-1-yl]ethyl acetate
31	11.402	0.0841	508.2642	$C_{23}H_{36}N_6O_7$ 	Asparaginylthreonylphenylalanyllysine
32	11.497	1.2700	301.2985	$C_{18}H_{39}NO_2$ 	Safingol
33	11.644	6.1813	414.2043	$C_{24}H_{30}O_6$ 	4,4'-[1,10-Decanediy]bis(oxy) dibenzoic acid
34	11.781	0.9642	693.3952	$C_{34}H_{55}N_5O_{10}$ 	(2R,3S)-4-[[[(2S)-1-[(2S,4S)-4-Hydroxy-2-[[[(2S)-2-methyl-5-oxo-2,5-dihydro-1H-pyrrol-1-yl]carbonyl]-1-pyrrolidinyl]-3-methyl-1-oxo-2-butanyl] (methyl)amino]-3-[(N-methyl-N-[(2-methyl-2-propyl)oxy] carbonyl]-L-leucyl)amino]-4-oxo-2-butanyl oxoacetate
35	12.297	2.1360	598.4022	$C_{25}H_{50}N_{12}O_5$ 	N2-Acetyl-L-arginyl-L-valyl-L-lysyl-L-argininamide
36	12.497	0.0803	700.3621	$C_{35}H_{52}N_6O_5S$ 	N-(3-Amino-3-methylbutanoyl)-O-methyl-L-tyrosyl-N-[(1R,2S)-3-cyclohexyl-1-[(5S)-3-ethyl-2-oxo-1,3-oxazolidin-5-yl]-1-hydroxy-2-propanyl]-3-(1,3-thiazol-4-yl)-L-alaninamide
37	12.877	1.1958	531.3407	$C_{27}H_{49}NO_9$ 	(3R,4S,6S,9R,11R,12R,13S,14R)-6-[[[(2S,3R,4S,6S)-4-(Dimethylamino)-3-hydroxy-6-methyltetrahydro-2H-pyran-2-yl]oxy]-14-ethyl-4,12,13-trihydroxy-3,9,11,13-tetramethyloxacyclotetradecane-2,10-dione (non-p referred name)
38	12.993	1.1111	671.4090	$C_{44}H_{53}N_3O_3$ 	1,2,9-Triheptyl-1,2-dihydroisoquinolino[4'5':6'6',5,10]anthra[2,1,9-def]cinnoline-3,8,10(9H)-trione

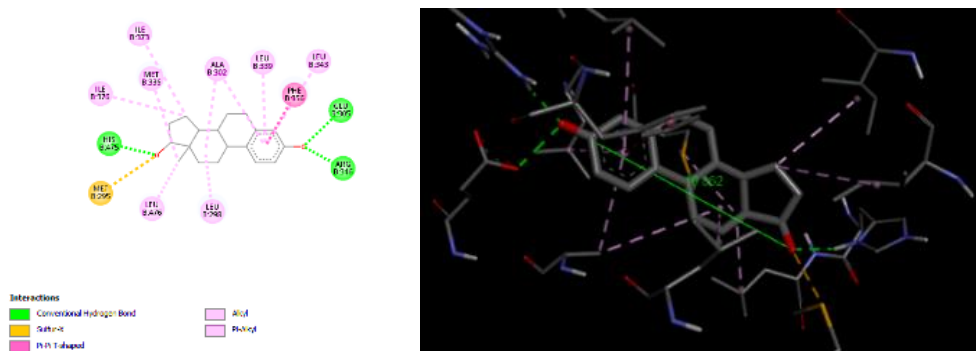
39	13.193	14.0522	495.3313		<chem>C26H45N3O6</chem>	1-(β-D-Arabinofuranosyl)-4-(heptadecanoylamino)-2(1H)-pyrimidinone
40	13.646	2.6446	473.3724		<chem>C22H48N9Cl</chem>	N2-[3-((12-((3-aminopropyl)amino)dodecyl)amino)propyl]-N4-methyl-1,3,5-triazine-2,4,6-triamine hydrochloride (1:1)
41	13.951	18.2182	473.3770		<chem>C32H47N3</chem>	(2R)-N-Benzyl-2-((3S)-3-benzyl-4-[2-(bicyclo[2.2.1]hept-2-yl)ethyl]-1-piperazinyl)-3-methyl-1-butanamine

The result of metabolite profiling showed a total of 79 compounds in dichloromethane and methanol solvents which consisted of 54 known and 25 unknown compounds. The use of the two solvents aimed at eluting the extract optimally in the column of UPLC-QToF-MS/MS<sup>27</sup>. The compound peak analyzed from the result of metabolite profiling was the RT peak between 0 and 14 minutes. The RT peak above 14 minutes could not be considered because the peak was generally impure, like the peak produced from solvent or degradant. From the total of detected 79 compounds, not all peaks in TIC could be identified in the process of metabolite profiling. This was shown by the appearance of 25 unknown compounds. Unknown compounds could not be identified in the database; these compounds could be in the form of impure compounds or degradant which were still detected by the instrument or new compounds which were still not listed in the database, especially unknown compounds which had high content<sup>27,46</sup>.

#### *In silico study*

The 79 compounds from metabolite profiling of 96% ethanol extract of the controlled environmental growth *M. crenata* leaves were then analyzed through molecular docking using PyRx 0.8 software and AutoDock Vina as the docking simulator. Based on the native ligand test (17β-estradiol) using 3OLS protein, the value of RMSD 1.238 Å was retrieved, which showed that RMSD <2 Å means the docking protocol could be used in the docking process of resulting compounds from metabolite profiling using 3OLS protein<sup>47,48</sup>. After that, the bond between native ligand and compound towards 3OLS protein was visualized using Biovia Discovery Visualizer 2016 software. Based on the analysis of molecular docking 17β-estradiol result on 3OLS protein, it was found that the compound was categorized as an ERβ agonist compound if it met several parameters similar to 17β-estradiol. These parameters consisted of a pharmacophore cluster that bonded His 475 amino acid to Glu 305 amino acid or Arg 346 amino acid, which can be viewed in **Figure 4**. The type of bond to the amino acid also influences the bonds' stability. This interaction describes the binding strength of the ligand to the receptor. The

hydrogen bonds can stabilize the interaction between ligands and receptors, in addition to van der Waals and electrostatic bonds<sup>49</sup>. Besides, they also had a pharmacophore distance similar to 17 $\beta$ -estradiol, approximately 10.862 Å. The similarity in pharmacophore distance from pharmacophore cluster on 17 $\beta$ -estradiol could be used as a guideline to predict other compounds with the same pharmacological effects<sup>50-52</sup>. The analysis using Discovery Studio Visualizer 2016 of 79 compounds resulted from metabolite profiling of 96% ethanol extract of the controlled environmental growth of *M. crenata* leaves can be seen in **Table IV**.



**Figure 4.** Interaction of 17 $\beta$ -estradiol with 3OLS protein.

**Table IV.** 17 $\beta$ -estradiol and compounds in 96% ethanol extract of *M. crenata* leaves which are agonists against ER $\beta$

No.	Compound Name	% Area	Binding Affinity (kcal/mol)	Amino Acid (Type of Bond)	Pharmacophore Distance (Å)
-	17 $\beta$ -estradiol	-	-10.5	His 475 (Hydrogen) Glu 305 (Hydrogen) Arg 346 (Hydrogen)	10.862
1	Methyl 2-([4-amino-6-(1-piperidinyl)-1,3,5-triazin-2-yl]methyl)sulfanyl)benzoate	1.5705	-3.8	His 475 (Pi-Alkyl) Glu 305 (Carbon)	8.596
2	N <sup>''</sup> ,N <sup>''''</sup> -(5-Methyl-2,4-pyrimidinediyl)dicarbohydrazonic diamide	0.3745	-7.1	His 475 (Unfavorable) Arg 346 (Unfavorable) Glu 305 (Salt Bridge)	9.521
3	N-[(E)-Amino[2-(1-hydrazono-2-propanylidene)hydrazino]methylene]acetamide	0.0311	-3.6	His 475 (Unfavorable) Glu 305 (Attractive Charge)	6.649
4	N-(4-Methyl-2-pentanyl)-N-phenyl-1,4-benzenediamine	0.2128	-7.9	His 475 (Alkyl) Glu 305 (Hydrogen)	10.05
5	7-(2-Methoxyethyl)-3-methyl-8-(1-pyrrolidinyl)-3,7-dihydro-1H-purine-2,6-dione	0.7608	-4.5	His 475 (Pi-Alkyl) Glu 305 (Hydrogen)	7.898
6	N-Cycloheptyl-2-methoxy-4-(methylsulfanyl) benzamide	0.3141	-2.2	His 475 (Unfavorable) Arg 346 (Sulfur)	11.430
7	Miserotoxin	0.7979	-6.1	His 475 (Unfavorable) Glu305 (Carbon) Arg 346 (Hydrogen)	10.377
8	(2-Methyl-2H-tetrazol-5-yl)methyl carbamo hydrazonothioate	0.6768	-5.3	His 475 (Unfavorable) Glu 305 (Carbon)	8.124

9	2,2-Dioxido-3,6,9-trioxa-2λ6-thiaundecan-11-yl ethyl (2E)-2-butenedioate	0.7756	-3.5	His 475 (Hydrogen) Arg 346 (Hydrogen)	10.887
10	(-)-Metanephine glucuronide	0.1558	-2.8	His 475 (Hydrogen) Glu 305 (Hydrogen)	10.377
11	3-(Ethylsulfonyl)-N-methyl-N-[3-(methylamino)propyl]-4-thiomorpholinesulfonamide	0.7356	-5.6	His 475 (Hydrogen) Glu 305 (Hydrogen)	8.436
12	2-[[4-Ethyl-5-(2-thienyl)-4H-1,2,4-triazol-3-yl]sulfonyl]-N-(2-methoxydibenzo[b,d]furan-3-yl)acetamide	0.4942	1.9	His 475 (Unfavorable) Glu 305 (Unfavorable)	10.936
13	(1S,4S)-1,4-Dihydronaphthalene-1,4-diylbis(methylene) bis(4-methylbenzenesulfonate)	1.1176	4	His 475 (Hydrogen) Glu305 (Unfavorable) Arg 346 (Hydrogen)	11.179
14	3',5'-Di-O-acetyl-2'-deoxy-5-[3-(3-nitrophenyl)-4-oxo-1,3-thiazolidin-2-yl]uridine	0.4796	20.1	His 475 (Hydrogen) Glu 305 (Unfavorable)	10.025
15	1,5-Anhydro-2,6-bis-O-(3,4,5-trihydroxybenzoyl) -1-[2,4,6-trihydroxy-3-(4-hydroxybenzoyl)phenyl]hexitol	0.0409	85.6	His 475 (Pi-Sigma) Glu 305 (Attractive charge)	10.019
16	Ethyl 3-(7-butoxy-6-chloro-4-methyl-2-oxo-2H-chromen-3-yl)propanoate	0.0231	-4.5	His 475 (Hydrogen) Glu 305 (Carbon)	10.063
17	3,4,5-Tris-O-[(2E)-3-(3,4-dihydroxyphenyl)-2-propenoyl]-D-glucaric acid	0.5161	20.4	His 475 (Hydrogen) Glu 305 (Hydrogen) Arg 346 (Hydrogen)	11.026
18	N2-Acetyl-L-arginyl-L-valyl-L-lysyl-L-argininamide	2.1360	11.1	His 475 (Unfavorable) Glu 305 (Hydrogen)	10.268
19	N-(3-Amino-3-methylbutanoyl)-O-methyl-L-tyrosyl-N-((1R,2S)-3-cyclohexyl-1-[(5S)-3-ethyl-2-oxo-1,3-oxazolidin-5-yl]-1-hydroxy-2-propanyl)-3-(1,3-thiazol-4-yl)-L-alaninamide	0.0803	26.3	His 475 (Unfavorable) Glu 305 (Hydrogen)	12.6

The result of *in silico* analysis showed that 19 compounds had the agonist characteristics towards 3OLS protein, which meant that those compounds belonged to phytoestrogen. To predict the compound potential as oral medicine, ERβ agonist compounds were then selected using the SwissADME web tool to identify the physicochemical properties of the compounds (The result of the SwissADME test can be seen on <https://doi.org/10.5281/zenodo.6904891>). The parameters used in the physicochemical analysis were molecule weight < 500 g/mol, HBD (hydrogen binding donors) < 5, HBA (hydrogen binding acceptors) < 10, TPSA ≤ 140 Å<sup>3</sup>, met Lipinski rule of five<sup>54</sup>, and BBB permeant "yes"<sup>55</sup>. The TPSA value showed the compounds' capability to penetrate the cell membrane, and the BBB permeant showed the compound's capability to penetrate the blood-brain barrier<sup>53,55</sup>. Lipinski's rule of five was used to predict the similarity of compounds and medicine, which had a specific biological activity designed for oral treatment<sup>53</sup>.

The analysis result of the TPSA parameter found 11 compounds that met those criteria. Based on the analysis of the Lipinski rule of five, it was found that 14 compounds met those criteria. At the same time, the analysis result of the BBB permeant parameter found that three compounds met those criteria. This indicates that these three compounds may influence the



CNS. Thus, the result of the physicochemical analysis showed that three ER $\beta$  agonist compounds met all parameters: TPSA, Lipinski rule of five, and BBB permeant, which can be seen in **Table V**.

**Table V.** Agonist compound that met all parameters of physicochemical analysis

No.	Compound name	Molecule weight (g/mol)	HBD	HBA	BBB Permeant	TPSA $\leq$ 140	Lipinski Rule of 5
1.	N-(4-Methyl-2-pentanyl)-N-phenyl-1,4-benzenediamine	268.40	1	0	Yes	29.26	Yes
2.	N-Cycloheptyl-2-methoxy-4-(methylsulfonyl)benzamide	293.42	1	2	Yes	63.63	Yes
3.	Ethyl 3-(7-butoxy-6-chloro-4-methyl-2-oxo-2H-chromen-3-yl)propanoate	366.84	0	5	Yes	65.74	Yes

The result of the physicochemical analysis above implied that those compounds were categorized as phytoestrogen, which was indicated by the agonist interaction with 3OLS protein and had the potential to be developed as antineuroinflammatory medicine given orally, which was shown by meeting physicochemical analysis parameters<sup>56,57</sup>. The correlation of these research findings was to prove that 96% ethanol extract of the controlled environmental growth of *M. crenata* leaves had *in vitro* antineuroinflammatory activity, which was shown by a significant decrease in MHC II expression, and supported by the prediction of 19 secondary metabolite compounds as the result of metabolite profiling on 96% ethanol extract of the controlled environmental growth of *M. crenata* which had *in silico* antineuroinflammatory activity and three of those compounds had the potential to be developed as oral medicine. The correlation result showed that the use of cultivated *M. crenata* had the advantage of decreasing MHC II expression significantly and contained more active compounds because of external factors control which could affect the compound content of the plant<sup>58</sup>.

## CONCLUSION

The 96% ethanol extract of the environmental-controlled growth of *M. crenata* has an antineuroinflammatory activity through MHC II expression inhibition on HMC3 microglia cells, with an optimum concentration of 62.5  $\mu\text{g}/\text{mL}$  and a value of 97.458 AU. This extract was predicted to contain 19 phytoestrogen compounds with agonist characteristics on ER $\beta$ , and three met all parameters of physicochemical analysis, including BBB permeant.

## ACKNOWLEDGMENT

None.

## AUTHORS' CONTRIBUTION

All authors have an equal contribution in carrying out this study.

## DATA AVAILABILITY

The result of the SwissADME test can be seen on <https://doi.org/10.5281/zenodo.6904891>.

## CONFLICT OF INTEREST

The authors declare there is no conflict of interest in this research.

## REFERENCES

1. Kalhan M, Singhanian K, Choudhary P, Verma S, Kaushal P, Singh T. Prevalence of Menopausal Symptoms and its Effect on Quality of Life among Rural Middle Aged Women (40-60 Years) of Haryana, India. *Int J Appl Basic Med Res.* 2020;10(3):183-8. doi:10.4103/ijabmr.ijabmr\_428\_19
2. Webster AD, Finstad DA, Kurzer MS, Torkelson CJ. Quality of life among postmenopausal women enrolled in the Minnesota Green Tea Trial. *Maturitas.* 2018;108:1-6. doi:10.1016/j.maturitas.2017.10.013
3. Silva TR, Oppermann K, Reis FM, Spritzer PM. Nutrition in Menopausal Women: A Narrative Review. *Nutrients.* 2021;13(7):2149. doi:10.3390/nu13072149
4. Dalal PK, Agarwal M. Postmenopausal syndrome. *Indian J Psychiatry.* 2015;57(Suppl 2):S222-32. doi:10.4103/0019-5545.161483
5. Kwon HS, Koh SH. Neuroinflammation in neurodegenerative disorders: the roles of microglia and astrocytes. *Transl Neurodegener.* 2020;9(1):42. doi:10.1186/s40035-020-00221-2
6. Au A, Feher A, McPhee L, Jessa A, Oh S, Einstein G. Estrogens, inflammation and cognition. *Front Neuroendocrinol.* 2016;40:87-100. doi:10.1016/j.yfrne.2016.01.002
7. Matt SM, Johnson RW. Neuro-immune dysfunction during brain aging: new insights in microglial cell regulation. *Curr Opin Pharmacol.* 2016;26:96-101. doi:10.1016/j.coph.2015.10.009
8. Arcuri C, Mecca C, Bianchi R, Giambanco I, Donato R. The pathophysiological role of microglia in dynamic surveillance, phagocytosis and structural remodeling of the developing CNS. *Front Mol Neurosci.* 2017;10:191. doi:10.3389/fnmol.2017.00191
9. Prieto GA, Cotman CW. Cytokines and cytokine networks target neurons to modulate long-term potentiation. *Cytokine Growth Factor Rev.* 2017;34:27-33. doi:10.1016/j.cytogfr.2017.03.005
10. Radtke FA, Chapman G, Hall J, Syed YA. Modulating neuroinflammation to treat neuropsychiatric disorders. *Biomed Res Int.* 2017;2017:5071786. doi:10.1155/2017/5071786
11. Dong Y, Li X, Cheng J, Hou L. Drug development for alzheimer's disease: Microglia induced neuroinflammation as a target? *Int J Mol Sci.* 2019;20(3):558. doi:10.3390/ijms20030558
12. Wixey JA, Reinebrant HE, Buller KM. Post-insult ibuprofen treatment attenuates damage to the serotonergic system after hypoxia-ischemia in the immature rat brain. *J Neuropathol Exp Neurol.* 2012;71(12):1137-48. doi:10.1097/nen.0b013e318277d4c7
13. Garrido-Mesa N, Zarzuelo A, Gálvez J. Minocycline: Far beyond an antibiotic. *Br J Pharmacol.* 2013;169(2):337-52. doi:10.1111/bph.12139
14. Zheng X, Yue P, Liu L, Tang C, Ma F, Zhang Y, et al. Efficacy between low and high dose aspirin for the initial treatment of Kawasaki disease: Current evidence based on a meta-analysis. *PLoS One.* 2019;14(5):e0217274. doi:10.1371/journal.pone.0217274
15. Rietjens IMCM, Lousse J, Beekmann K. The potential health effects of dietary phytoestrogens. *Br J Pharmacol.* 2017;174(11):1263-80. doi:10.1111/bph.13622
16. Jantaratnotai N, Utaisincharoen P, Sanvarinda P, Thampithak A, Sanvarinda Y. Phytoestrogens mediated anti-inflammatory effect through suppression of IRF-1 and pSTAT1 expressions in lipopolysaccharide-activated microglia. *Int Immunopharmacol.* 2013;17(2):483-8. doi:10.1016/j.intimp.2013.07.013

17. Villa A, Vegeto E, Poletti A, Maggi A. Estrogens, neuroinflammation, and neurodegeneration. *Endocr Rev.* 2016;37(4):372–402. doi:10.1210/er.2016-1007
18. Ma'arif B, Fitri H, Saidah NL, Najib LA, Yuwafi AH, Atmaja RRD, et al. Prediction of compounds with antiosteoporosis activity in *Chrysophyllum cainito* L. leaves through in silico approach. *J Basic Clin Physiol Pharmacol.* 2021;32(4):803–8. doi:10.1515/jbcpp-2020-0393
19. Desmawati D, Sulastri D. Phytoestrogens and Their Health Effect. *Open Access Maced J Med Sci.* 2019;7(3):495-9. doi:10.3889/oamjms.2019.044
20. Liu T, Li N, Yan YQ, Liu Y, Xiong K, Liu Y, et al. Recent advances in the anti-aging effects of phytoestrogens on collagen, water content, and oxidative stress. *Phytother Res.* 2020;34(3):435-47. doi:10.1002/ptr.6538
21. Ma'arif B, Aditama AP. Activity of 96% Ethanol Extract of *Chrysophyllum Cainito* L. in Increasing Vertebrae Trabecular Osteoblast Cell Number in Male Mice. *Asian J Pharm Clin Res.* 2019;12(1):286-8. doi:10.22159/ajpcr.2019.v12i1.28994
22. Agil M, Laswati H, Kuncoro H, Ma'arif B. In silico Analysis of Phytochemical Compounds in Ethyl Acetate Fraction of Semanggi (*Marsilea crenata* Presl.) Leaves As Neuroprotective Agent. *Res J Pharm Technol.* 2020;13(8):3745–52. doi:10.5958/0974-360x.2020.00663.0
23. Putra HL. Green clover Potentiates Delaying the Increment of Imbalance Bone Remodeling Process in Postmenopausal Women. *Folia Medica Indonesiana.* 2011;47(2):112–7.
24. Nurjanah, Azka A, Abdullah A. Aktivitas Antioksidan Dan Komponen Bioaktif Semanggi Air (*Marsilea Crenata*). *Asian J Innov Entrep.* 2012;1(3):152–8. doi:10.20885/ajie.vol1.iss3.art2
25. Ma'arif B, Agil M, Laswati H. Phytochemical Assessment on N-Hexane Extract and Fractions of *Marsilea crenata* Presl. Leaves through GC-MS. *Trad Med J.* 2016;21(2):77–85. doi:10.22146/tradmedj.12821
26. Ma'arif B, Agil M, Laswati H. Alkaline phosphatase activity of *Marsilea crenata* Presl. extract and fractions as marker of MC3T3-E1 osteoblast cell differentiation. *J Appl Pharm Sci.* 2018;8(3):55–9. doi:10.7324/JAPS.2018.8308
27. Ma'arif B, Mirza DM, Suryadinata A, Muchlisin MA, Laswati H, Agil M. Metabolite Profiling of 96% Ethanol Extract from *Marsilea crenata* Presl. Leaves Using UPLC-QToF-MS/MS and Anti-Neuroinflammatory Prediction Activity with Molecular Docking. *J Trop Pharm Chem.* 2019;4(6):261–70. doi:10.25026/jtpc.v4i6.213
28. Ma'arif B, Agil M, Laswati H. The enhancement of Arg1 and activated ER $\beta$  expression in microglia HMC3 by induction of 96% ethanol extract of *Marsilea crenata* Presl. leaves. *J Basic Clin Physiol Pharmacol.* 2019;30(6):20190284. doi:10.1515/jbcpp-2019-0284
29. Agil M, Kusumawati I, Purwitasari N. Phenotypic Variation Profile of *Marsilea crenata* Presl. Cultivated in Water and in the Soil. *J Botany.* 2017;2017:7232171. doi:10.1155/2017/7232171
30. Opačić N, Radman S, Uher SF, Benko B, Voća S, Žlabur JŠ. Nettle Cultivation Practices-From Open Field to Modern Hydroponics: A Case Study of Specialized Metabolites. *Plants.* 2022;11(4):483. doi:10.3390/plants11040483
31. Fussy A, Papenbrock J. An Overview of Soil and Soilless Cultivation Techniques-Chances, Challenges and the Neglected Question of Sustainability. *Plants.* 2022;11(9):1153. doi:10.3390/plants11091153
32. Chen SL, Yu H, Luo HM, Wu Q, Li CF, Steinmetz A. Conservation and sustainable use of medicinal plants: Problems, progress, and prospects. *Chin Med.* 2016;11:37. doi:10.1186/s13020-016-0108-7
33. Ma'arif B, Suleman HF, Annisa R, Dianti MR, Laswati H, Agil M. Efek Antineuroinflamasi Ekstrak Etanol 96% Daun *Marsilea crenata* Presl. Budidaya Papda Sel Mikroglia HMC3. *J Farmasi Udayana.* 2020;9(2):91-9. doi:10.24843/JFU.2020.v09.i02.p04

34. Engler-Chiurazzi EB, Brown CM, Povroznik JM, Simpkins JW. Estrogens as neuroprotectants: Estrogenic actions in the context of cognitive aging and brain injury. *Prog Neurobiol.* 2017;157:188–211. doi:10.1016/j.pneurobio.2015.12.008
35. Muchtaridi M, Dermawan D, Yusuf M. Molecular docking, 3D structure-based pharmacophore modeling, and ADME prediction of alpha mangostin and its derivatives against estrogen receptor alpha. *J Young Pharm.* 2018;10(3):252–9. doi:10.5530/jyp.2018.10.58
36. Rettberg J, Yao J, Brnton R. Estrogen: A master regulator of bioenergetic systems in the brain and body. *Front Neuroendocrinol.* 2014;35(1):515–25. doi:10.1016/j.yfrne.2013.08.001
37. Tang Y, Le W. Differential Roles of M1 and M2 Microglia in Neurodegenerative Diseases. *Mol Neurobiol.* 2016;53(2):1181–94. doi:10.1007/s12035-014-9070-5
38. Papageorgiou IE, Lewen A, Galow LV, Cesetti T, Scheffel J, Regen T, et al. TLR4-activated microglia require IFN- $\gamma$  to induce severe neuronal dysfunction and death in situ. *Proc Natl Acad Sci U S A.* 2016;113(1):212–7. doi:10.1073/pnas.1513853113
39. Cherry JD, Olschowka JA, O'Banion MK. Neuroinflammation and M2 microglia: The good, the bad, and the inflamed. *J Neuroinflammation.* 2014;11:98. doi:10.1186/1742-2094-11-98
40. Shih RH, Wang CY, Yang CM. NF-kappaB signaling pathways in neurological inflammation: A mini review. *Front Mol Neurosci.* 2015;8:77. doi:10.3389/fnmol.2015.00077
41. Vandenberg LN, Colborn T, Hayes TB, Heindel JJ, Jacobs DR, Lee DH, et al. Hormones and endocrine-disrupting chemicals: Low-dose effects and nonmonotonic dose responses. *Endocr Rev.* 2012;33(3):378–455. doi:10.1210/er.2011-1050
42. Lagarde F, Beausoleil C, Belcher SM, Belzunces LP, Emond C, Guerbet M, et al. Non-monotonic dose-response relationships and endocrine disruptors: A qualitative method of assessment. *Environ Health.* 2015;14:13. doi:10.1186/1476-069x-14-13
43. Balouiri M, Sadiki M, Ibensouda SK. Methods for in vitro evaluating antimicrobial activity: A review. *J Pharm Anal.* 2016;6(2):71–9. doi:10.1016/j.jpha.2015.11.005
44. Lu J, Muhmood A, Czekala W, Mazurkiewicz J, Dach J, Dong R. Untargeted metabolite profiling for screening bioactive compounds in digestate of manure under anaerobic digestion. *Water.* 2019;11(11):2420. doi:10.3390/w11112420
45. Duarte AJ, Ribeiro D, Moreira L, Amaral O. In silico analysis of missense mutations as a first step in functional studies: Examples from two sphingolipidoses. *Int J Mol Sci.* 2018;19(11):3409. doi:10.3390/ijms19113409
46. Aditama APR, Ma'arif B, Mirza DM, Laswati H, Agil M. In vitro and in silico analysis on the bone formation activity of N-hexane fraction of Semanggi (*Marsilea crenata* Presl.). *Syst Rev Pharm.* 2020;11(11):837–49.
47. Kartika IGAA, Bang IJ, Riani C, Insanu M, Kwak JH, Chung KH, et al. Isolation and Characterization of Phenylpropanoid and Lignan Compounds from *Peperomia pellucida* [L.] Kunth with Estrogenic Activities. *Molecules.* 2020;25(21):4914. doi:10.3390/molecules25214914
48. Pinto VdS, Araújo JSC, Silva RC, da Costa GV, Cruz JN, Neto MFDA, et al. In silico study to identify new antituberculosis molecules from natural sources by hierarchical virtual screening and molecular dynamics simulations. *Pharmaceuticals.* 2019;12(1):36. doi:10.3390/ph12010036
49. Chen D, Oezguen N, Urvil P, Ferguson C, Dann SM, Savidge TC. Regulation of protein-ligand binding affinity by hydrogen bond pairing. *Sci Adv.* 2016;2(3):e1501240. doi:10.1126/sciadv.1501240

50. Sellami A, Montes M, Lagarde N. Predicting Potential Endocrine Disrupting Chemicals Binding to Estrogen Receptor  $\alpha$  (ER $\alpha$ ) Using a Pipeline Combining Structure-Based and Ligand-Based in Silico Methods. *Int J Mol Sci.* 2021;22(6):2846. doi:10.3390/ijms22062846
51. Vourinen A, Engeli R, Meyer A, Bachmann F, Griesser UJ, Schuster D, et al. Ligand-based pharmacophore modeling and virtual screening for the discovery of novel 17 $\beta$ -hydroxysteroid dehydrogenase 2 inhibitors. *J Med Chem.* 2014;57(14):5995-6007. doi:10.1021/jm5004914
52. Kaserer T, Beck KR, Akram M, Odermatt A, Schuster D. Pharmacophore Models and Pharmacophore-Based Virtual Screening: Concepts and Applications Exemplified on Hydroxysteroid Dehydrogenases. *Molecules.* 2015;20(12):22799-832. doi:10.3390/molecules201219880
53. Truong J, George A, Holien JK. Analysis of physicochemical properties of protein-protein interaction modulators suggests stronger alignment with the "rule of five". *RSC Med Chem.* 2021;12(10):1731-49. doi:10.1039/d1md00213a
54. Benet LZ, Hosey CM, Ursu O, Oprea TI. BDDCS, the Rule of 5 and Drugability. *Adv Drug Deliv Rev.* 2016;101:89-98. doi:10.1016/j.addr.2016.05.007
55. Geldenhuys WJ, Mohammad AS, Adkins CE, Lockman PR. Molecular determinants of blood-brain barrier permeation. *Ther Deliv.* 2015;6(8):961-71. doi:10.4155/tde.15.32
56. Daina A, Zoete V. A BOILED-Egg To Predict Gastrointestinal Absorption and Brain Penetration of Small Molecules. *ChemMedChem.* 2016;11(11):1117-21. doi:10.1002/cmdc.201600182
57. Chagas CM, Moss S, Alisaraie L. Drug metabolites and their effects on the development of adverse reactions: Revisiting Lipinski's Rule of Five. *Int J Pharm.* 2018;549(1-2):133-49. doi:10.1016/j.ijpharm.2018.07.046
58. Yang L, Wen KS, Ruan X, Zhao YX, Wei F, Wang Q. Response of plant secondary metabolites to environmental factors. *Molecules.* 2018;23(4):762. doi:10.3390/molecules23040762